

Tunneling Magneto-Resistance Effect of γ -Fe₄N with MgO Barrier

Yoshihide Kimishima, Koki Homma, Masatomo Uehara and Ryota Taninoki

Department of Physics, Faculty of Engineering, Graduate School of Yokohama National University,
Tokiwadai 79-5, Hodogaya, Yokohama 240-8501, Japan
Fax: +81-45-339-4182, e-mail: kimi@ynu.ac.jp

γ -Fe₄N is the ferromagnetic material with high Curie temperature and relatively high electrical conductivity. First principle calculation showed that the γ -Fe₄N was a half-metal by 100% spin polarized conduction electrons with minority spins. So we expected large tunneling magneto-resistance effect in the Fe₄N/MgO/Fe₄N junctions. γ -Fe₄N was prepared by sintering Fe₃O₄ nanoparticles in the atmosphere of NH₃/H₂ gas mixture at 673 K. Then MgO was added to the γ -Fe₄N powder and sintered at about 473 K in pure Ar gas. Magneto-resistance was measured by 4-terminals method for $x=0$ -0.8 samples of (MgO)_{*x*}(Fe₄N)_{1-*x*}, and magneto-resistance ratios of -1.2~-1 % were observed for $x=0.3$ -0.6 samples at 300K. It is the first observation of tunneling magneto-resistance effect for γ -Fe₄N granular system.

Key Words : γ -Fe₄N, MgO, magnetization, magneto-resistance, TMR

1. INTRODUCTION

Perovskite-type iron nitride γ -Fe₄N is a ferromagnet with a large magnetic moment below the Curie temperature T_c of 761 K [1], and has been considered as a promising material for magnetic recording media. The electronic structure of this compound has been calculated [2, 3], and a recent result for the spin polarization coefficient P [4] showed that this compound was a perfectly spin-polarized material with $P = -1$ at the Fermi level E_F . Here P was defined by $(\sigma_{\uparrow} - \sigma_{\downarrow}) / (\sigma_{\uparrow} + \sigma_{\downarrow})$, and σ_{\uparrow} and σ_{\downarrow} were the conductivities of up and down spin electrons, respectively. Thus Fe₄N is a candidate of spintronics material for magnetic random access memory (MRAM) etc.

Powder specimens of γ -Fe₄N have been prepared in atmospheres of NH₃+H₂ mixed gases from the precursors of Fe [5], FeCl₂ [6], Fe₂O₃ [7] and Fe₃O₄ nano-particles [8]. In particular, Wu *et al.* [8] revealed the gradual conversion of Fe₃O₄ into γ -Fe₄N by reduction and nitriding in NH₃+H₂ mixed gases between 673 K and 973 K. They reported the measured results of magnetization and permeability of four kinds of samples, which were sintered at 673 K, 773 K, 873 K, and 973 K, but did not report any magneto-resistance data.

In the previous studies, highly oriented or single-crystalline MgO was revealed as a good tunneling barrier for the polarized conduction electrons [9]. Therefore, the present authors are interested in the magneto-resistive behaviors of the Fe₄N/MgO granular system, and describe their experimental results for the magnetization, resistivity, and magneto-resistance in this paper.

2. SAMPLE PREPARATION

First, the precursors of Fe₃O₄ nano-particles were prepared from a mixed aqueous solution of FeCl₂·4H₂O and FeCl₃·6H₂O with the mole ratio of 1:2. When an aqueous ammonium solution (NH₄OH) was dripped onto

the above mixed solution, Fe₃O₄ nano-particles with a diameter of about 10 nm were precipitated [10-12]. Washed and dried Fe₃O₄ nano-particles were pressed to form pellets with a diameter of 10 mm, and sintered in the NH₃+H₂ mixed gases for 12 hours at 673 K. Then the mixtures of prepared γ -Fe₄N specimen and MgO powder were sintered at 473K for 3 hours in air.

Powder CuK α X-ray diffraction (XRD) patterns of (MgO)_{*x*}(Fe₄N)_{1-*x*} samples are shown in Fig. 1, where x is the mol ratio of MgO. The crystal structure of γ -Fe₄N is a cubic perovskite with the lattice parameter of $a = 0.379$ nm [13], while MgO has a NaCl structure with $a = 0.4211$ nm [14].

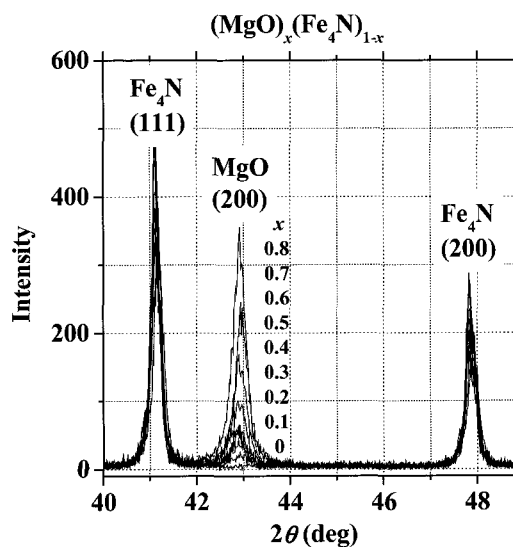


Fig. 1 XRD patterns of (MgO)_{*x*}(Fe₄N)_{1-*x*} samples from $x=0$ to 0.8.

From the half width of each diffraction peak, the mean diameter d of Fe_4N and MgO particles were estimated by Sherrer's formula as about 80 nm and 30 nm, respectively.

3. EXPERIMENTAL RESULTS AND DISCUSSION

3.1 Magnetization

The magnetization M was measured by means of a vibrating sample magnetometer (VSM) between 77 K and 300 K. Fig. 2 shows the temperature dependence of M at 5 kOe. The magnitude of M monotonically decreases with the mole ratio x of MgO.

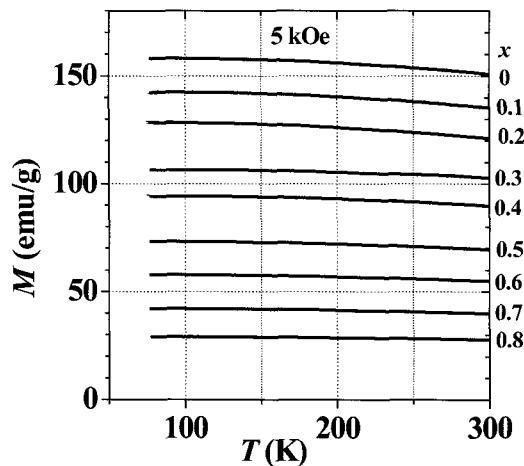


Fig. 2 Temperature dependence of the magnetization at 5 kOe, where x is the mole ratio of MgO.

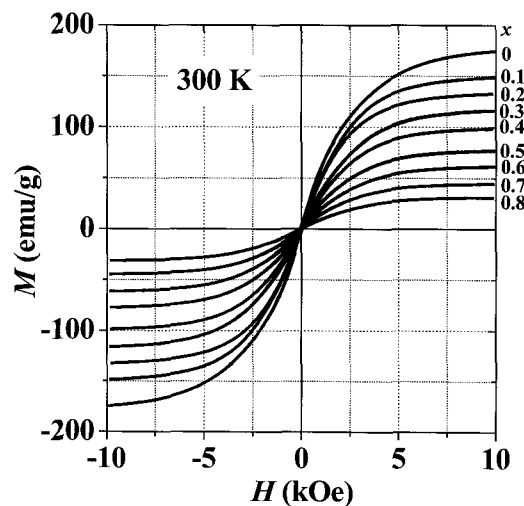


Fig. 3 Field dependence of the magnetization at 300 K, where x is the mole ratio of MgO.

Field dependences of magnetization M at 300 K are shown in Fig. 3. The saturation magnetization M_s at 77 K and 300 K were 189 emu/g and 179 emu/g, respectively for the $x = 0$ sample of pure $\gamma\text{-Fe}_4\text{N}$, as shown in Fig. 4. These values are considered to be reasonable when compared with data in the preceding literature [8, 15, 16].

The values of M_s decrease almost linearly with increasing x , obeying the relation of

$$M_s(x) = (1-x) M_s(0) \quad (1).$$

It shows that non-interactive coexistence of $\gamma\text{-Fe}_4\text{N}$ and MgO phase is realized in each sample. The coercive fields H_c 's were about 50 Oe and 90 Oe at 300 K and 77 K, respectively, for all of the samples.

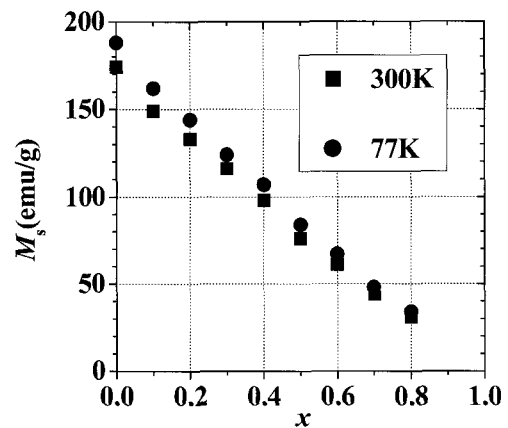


Fig. 4 x -dependence of the saturation magnetization at 300 K and 77 K.

3.2 Resistivity

Resistivity ρ was measured by the four-terminals dc method between 77 K and 300 K. The $T^{-1/2}$ dependences of ρ are plotted in Fig. 5 by means of a semi-logarithmic scale.

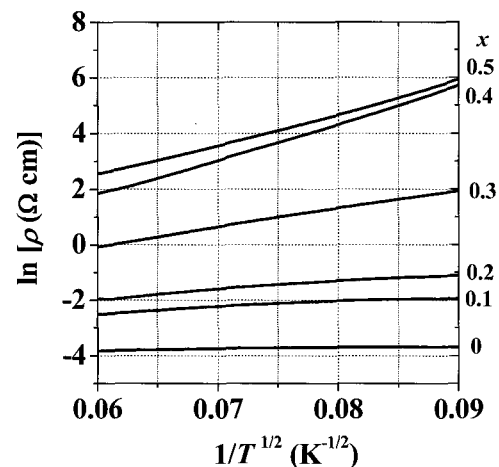


Fig. 5 $T^{-1/2}$ dependences of ρ plotted by means of a semi-logarithmic scale.

For an $x = 0$ sample of pure $\gamma\text{-Fe}_4\text{N}$, weakly semi-conductive behavior appears in the $\rho(T)$ -curve. It was assumed that the magnitude of ρ monotonically increased with x , because MgO was an insulator with very high ρ . As shown in Fig. 5, ρ drastically

increased with increasing x . In addition, the linearity of $\ln \rho$ to $T^{-1/2}$ appears for the sample above $x = 0.1$. The tunneling magneto-resistance (TMR) theory [17, 18] gives the following expression for the resistivity of a granular system.

$$\rho = \frac{\rho_0}{1 + P^2 m^2} \exp\left(\sqrt{\frac{\Delta}{T}}\right) \quad (2),$$

where ρ_0 and Δ are constants, P is the spin polarization coefficient of conduction electrons, and m is defined by M/M_s . The parameter Δ is defined by $8\kappa C$, where $C = sE_c = \text{const.}$ and $\kappa = \sqrt{2m^*(V - E_F)/\hbar^2}$. The parameter m^* is the effective mass of electrons, V is the barrier potential, E_F is the Fermi energy, s is the barrier thickness, and E_c is the charging energy.

The linear dependence of $\ln \rho$ on $T^{-1/2}$ shows that the MgO grains form good TMR barriers, and the increasing gradient of $\ln \rho$ vs. $T^{-1/2}$ curve means that the barrier potential is enlarged by the increasing of Mg content x .

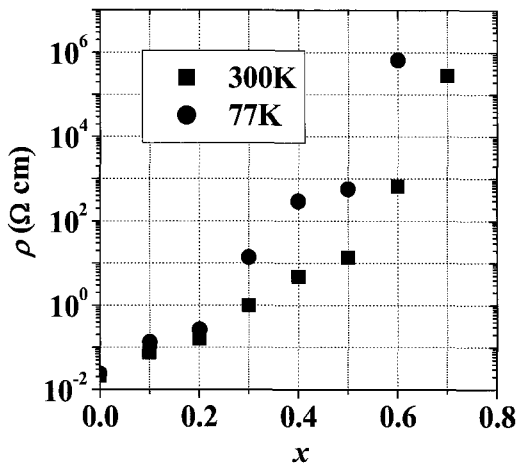
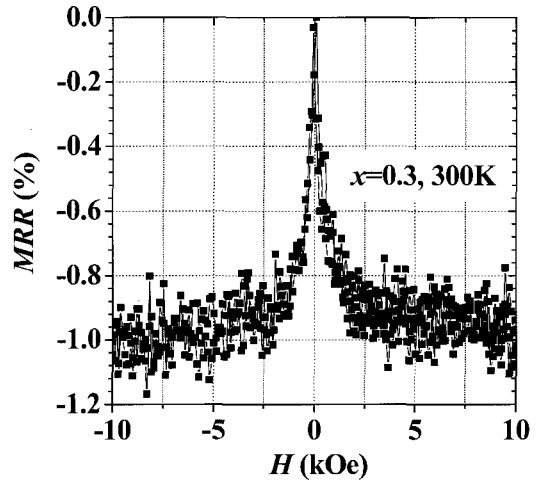


Fig. 6 x -dependence of the resistivity ρ at 300K and 77K.

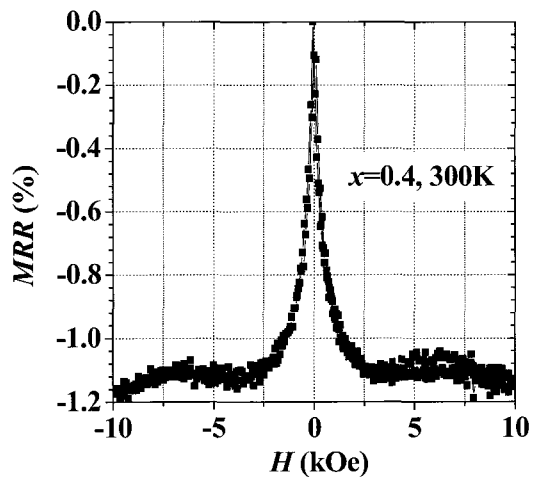
The x -dependences of ρ at 300 K and 77 K are shown in Fig. 6 by a semi-logarithmic scale, where ρ rapidly increases above $x = 0.3$. If x reaches near the percolation threshold [19, 20], the conducting paths of γ -Fe₄N begin to disconnect from end to end of the sample. Therefore we can assume that the percolation threshold x_c is above 0.3. In this x -region, the connectivity of γ -Fe₄N grains becomes very weak and the MgO grains with high resistivity between γ -Fe₄N particles play an important role. The present system, including optimum tunneling barriers of MgO, should exhibit large TMR, since the linear change of $\ln \rho$ with $T^{-1/2}$ supports the notion that good TMR junctions are formed.

3.3 Magneto-resistance

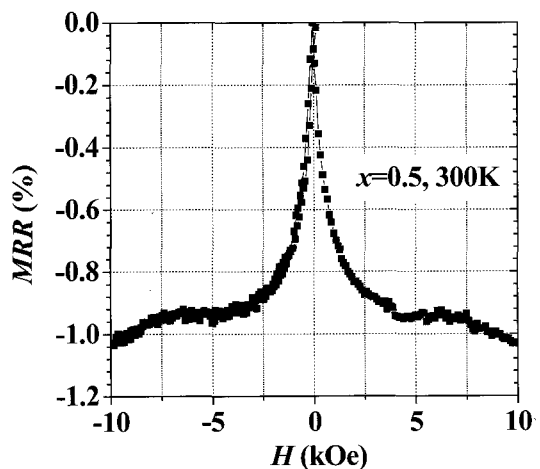
The field dependence of the resistivity $\rho(H)$ was measured between -10 kOe and 10 kOe at 300 K and 77 K, and the experimental results of the magneto-resistance ratio (MRR) are shown in Fig. 7(a)-(d) for $x = 0.3, 0.4, 0.5$ and 0.6 samples. Here the MRR is defined by



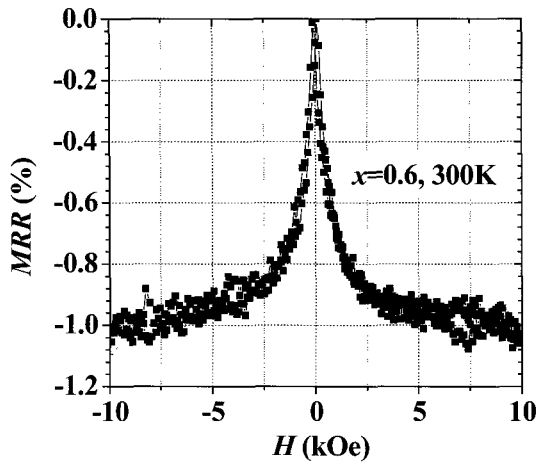
(a)



(b)



(c)



(d)

Fig. 9 Field dependence of the magneto-resistance ratio MRR at 300 K for $x = 0.3$ (a), $x = 0.4$ (b), $x = 0.5$ (c), $x = 0.6$ (d).

$[\rho(H) - \rho(H_p)] / \rho(H_p)$, where H_p is the peak field at which $\rho(H)$ becomes maximum. In the case of TMR, the H_p is generally consistent with coercive field H_c of ferromagnetic parts.

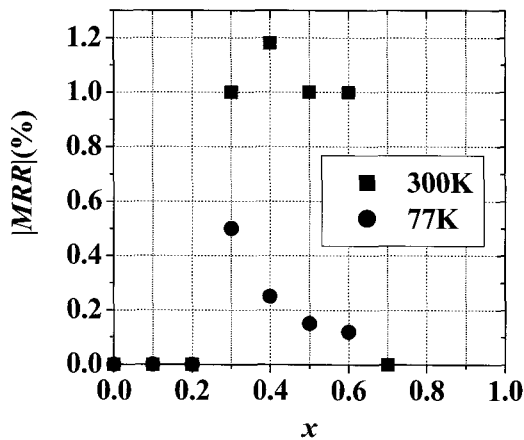


Fig. 8 x -dependences of MRR at 300 K and 77 K.

The x -dependences of MRR at 300 K and 77 K are shown in Fig. 8. The MRR 's were apparently observed only for $x=0.3-0.6$ samples, where the values of $|MRR|$ are 1-1.2 % at 300 K, and 0.2-0.5 % at 77 K. The value of $|MRR|$ at room temperature may be due to the tunneling barriers of MgO at the inter-grain part between γ -Fe₄N grains. It is the first observation of TMR effect for γ -Fe₄N granular system. Peak values of $|MRR|$ near the percolation threshold has also been reported for half-metallic CrO₂ with TiO₂ [21] and polymer barriers [22] at 77 K.

4. CONCLUSION

Mixtures of $(MgO)_x(\gamma\text{-Fe}_4\text{N})_{1-x}$ were prepared from

commercial MgO and γ -Fe₄N from Fe₃O₄ nanoparticles in NH₃+H₂ mixed gases. The magnetization M and the saturation magnetization of M_s could be explained by the non-interactive co-existence of γ -Fe₄N and MgO phase in each sample. The temperature and field dependence of the resistivity showed that good TMR junctions were formed at $x = 0.3-0.6$ near the percolation threshold. Relatively large $|MRR|$ values of 1-1.2 % were observed at room temperature, which may be due to the effective TMR barriers of MgO in the grain boundaries between γ -Fe₄N particles. It is the first observation of TMR effect for γ -Fe₄N granular system.

REFERENCES

- [1] C. Guillaud, and H. Creveaux, *Compt. Rend.*, **222**, 1170-72 (1946).
- [2] A. Sakuma, *J. Magn. Magn. Mat.*, **102**, 127-34 (1991).
- [3] A. Sakuma, *J. Phys. Soc. Jpn.*, **60**, 2007-12 (1991).
- [4] S. Kokado, N. Fujima, K. Harigaya, H. Shimizu, and A. Sakuma, *Phys. Rev. B*, **73**, 172410-1-4 (2006).
- [5] K. Tagawa, E. Kita, and A. Tasaki, *Jpn. J. Appl. Phys.*, **21**, 1596-98 (1982).
- [6] M. Cao, R. Wang, X. Fang, Z. Cui, T. Chang, and H. Yang, *Powder Technol.*, **115**, 96-98 (2001).
- [7] C.A. Grimes, D. Qian, E.C. Dickey, J.L. Allen, and P.C. Eklund, *J. Appl. Phys.*, **87**, 5642-44(2004).
- [8] X. L. Wu, W. Zhong, H. Y. Jiang, N. J. Tang, W. Q. Zou, and Y. W. Du, *J. Magn. Magn. Mat.*, **281**, 77-81 (2004).
- [9] S. Yuasa, T. Nagahama, A. Fukushima, Y. Suzuki and K. Ando, *Nature Materials*, **3**, 868-871 (2004).
- [10] Y. Kimishima, M. Uehara, Y. Notani, K. Kobayashi, and W. Yamada, *Trans. Mat. Res. Soc. Jpn.*, **29**, 1543-46 (2004).
- [11] Y. Kimishima, W. Yamada, K. Kobayashi, M. Uehara, T. Asaka, K. Kimoto, and Y. Matsui, *Trans Magn. Soc. Jpn.*, **5**, 73-76 (2005).
- [12] Y. Kimishima, W. Yamada, M. Uehara, T. Asaka, K. Kimoto, and Y. Matsui, *Mat. Sci. Eng. B.*, **138**, 69-73 (2007).
- [13] H. Jacobs, D. Rechenbach, and U. Zachwieja, *J. Alloys Compds.*, **227**, 10-17 (1995).
- [14] R.W.G. Wyckoff, *Crystal Structures* 2nd edition, Inter-science, New York, (1965).
- [15] B.C. Frazer, *Phys. Rev.*, **112**, 751-54 (1958).
- [16] L.L. Wang, X. Wang, N. Ma, W.T. Zheng, D.H. Jin, and Y.Y. Zhao, *Surf. Coat. Technol.*, **201**, 786-91 (2006).
- [17] P. Sheng, B. Abeles, and Y. Arie, *Phys. Rev. Lett.*, **31**, 44-47 (1973).
- [18] J. Inoue, and S. Maekawa, *Phys. Rev. B*, **53**, R11927-29 (1996).
- [19] V. K. Shante, and S. Kirkpatrick: *Adv. Phys.*, **20**, 325-57 (1971).
- [20] J. P. Straley: *Phys. Rev. B*, **15**, 5733-37 (1977).
- [21] Y-J. Chen, X-Y. Zhang, T-Y. Cai, and Z-Y. Li, *Mat. Lett.*, **58**, 262-66 (2003).
- [22] Y-J. Chen, X-Y. Zhang, and Z-Y. Li, *Chem. Phys. Lett.*, **375**, 213-18 (2003).

(Received December 5, 2007 ; Accepted March 12, 2008)